Superparamagnetic resonance of annealed iron-containing borate glass

1998 J. Phys.: Condens. Matter 10 8559

(http://iopscience.iop.org/0953-8984/10/38/016)

J. Phys.: Condens. Matter **10** (1998) 8559–8572. Printed in the UK PII: S0953-8984(98)94867-6

Superparamagnetic resonance of annealed iron-containing borate glass

René Berger†§, Janis Kliava†, Jean-Claude Bissey† and Vanessa Baïetto‡

† Centre de Physique Moléculaire Optique et Hertzienne, UMR Université Bordeaux I-CNRS 5798, 351 cours de la Libération, 33405 Talence Cedex, France

‡ Centre de Recherche en Physique Appliquée à l'Archéologie, UPRESA CNRS 5060, Université Michel de Montaigne, Esplanade des Antilles, 33405 Talence Cedex, France

Received 8 June 1998, in final form 13 July 1998

Abstract. A lithium borate glass containing a small amount of iron oxide is studied by electron magnetic resonance at room temperature after repeated annealing steps between 460 and 670 °C. As the anneal temperature increases, the $g_{ef} = 4.3$ sharp line characteristic of isolated iron ions decreases in intensity and finally disappears. Simultaneously, a narrow line emerges at $g_{ef} \approx 2.0$, superposed with a broader one, the narrow and the broader components predominating respectively after annealing at lower and at higher temperatures. Computer simulations of spectra have been carried out, based on a model of resonance of ferromagnetic single-domain nanoparticles randomly dispersed in the devitrified glass (superparamagnetic resonance). As the anneal temperature increases, the most probable particle diameter obtained assuming a log–normal distribution of diameters increases from 2.9 to 4.7 nm showing a saturation at higher anneal temperatures, whereas the relative number of larger particles grows continuously.

1. Introduction

In glass technology crystallization must usually be avoided; however, partially crystallized glasses or 'glass-ceramics', containing fine crystallized particles (nanoparticles), have been developed for specific applications. These nanoparticles confer particular characteristics to glasses, such as strength and impact resistance, lower thermal expansion coefficient, partial or complete opacity, etc [1]. A special type of nanoparticles, ferro- or ferrimagnetically ordered crystalline nanoparticles imbedded in different diamagnetic matrices such as fluids or polymers, gives rise to a new kind of magnetism called superparamagnetism and results in a number of properties which are interesting from a technical viewpoint, for example see [2].

Partially crystallized glasses containing ferromagnetic nanoparticles constitute a novel and much more complex class of superparamagnetic materials. Their properties are mainly determined by morphology (size and shape distributions) and magnetic constants of such particles. Electron magnetic resonance, sensitive to both the magnetic constants and the structure of the environment of a magnetic ion, is well adapted to the study of superparamagnetic nanoparticles [3]. In this case it may be called superparamagnetic resonance (SPR) to distinguish it from the resonance of individual electron spins usually referred to as electron paramagnetic resonance (EPR). Up until now, only a few attempts

§ Corresponding author. E-mail address: berger@frbdx11.cribx1.u-bordeaux.fr.

0953-8984/98/388559+14$19.50

have been made to carry out quantitative, computer-simulation based analysis of SPR spectra of magnetic particles dispersed in polycrystalline or glassy systems [3–5].

In a previous work [3] we have dealt with transformations arising in the electron magnetic resonance spectra of borate glasses containing small amounts of iron oxide after heat treatment above the glass transition temperature. Namely, the resonance characteristic of diluted Fe^{3+} ions in the glass, observed at the effective g-value $g_{ef} = 4.3$ [6], progressively disappears and a new resonance, consisting of superposed broader and narrower components, grows at $g_{ef} \approx 2.0$. This compound resonance signal has been ascribed to a superparamagnetic assembly of crystalline ferromagnetic single-domain particles arising in the diamagnetic glassy matrix under heat treatment. Good computer fits to this resonance have been obtained assuming a monodisperse distribution of the particle sizes.

This paper presents a more detailed analysis of room temperature X-band SPR spectra obtained after repeated annealing steps of iron-doped borate glass. First, data are reported on the evolution of the number of spins with annealing, as obtained from resonance intensity measurements. Then, geometrical characteristics of the magnetic particles obtained from a series of computer simulations of the spectra are related to the anneal temperature. Finally, the mechanism of growth of crystallized magnetic particles is discussed.

2. Experimental results

A glass of the initial composition $0.63B_2O_3$–$0.37Li_2O$–0.75×10^{-3} Fe_2O_3 was prepared from a mixture of B_2O_3, Li_2O and Fe_2O_3, melted in a platinum crucible and quenched in air. The low level of iron oxide in the melt was selected to avoid clustering of the iron ions prior to any heat treatment.

The glass transition temperature, $T_g = 435\,^{\circ}C$, was determined by differential scanning calorimetry. In heat treated glasses, the x-ray diffraction technique has detected only two crystalline phases: $LiBO_2$ and $Li_2B_4O_7$. No iron-containing phases could be directly observed, because of the very low iron content.

The glass sample was annealed in air by repeated stages in an electric furnace for 0.5 h at increasing anneal temperatures T_a ranging from 460 to 670 °C and cooled down to room temperature after each annealing step. The anneal temperature was calibrated with a relative uncertainty of 1%.

The resonance spectra were recorded at room temperature with an X-band (9.5 GHz) Varian spectrometer.

As reported earlier [7], at room temperature the X-band EPR spectrum of a non-annealed glass exhibits an asymmetric sharp line at $g_{ef} = 4.3$ accompanied by a plateau towards low magnetic fields down to $g_{ef} = 9.7$, which is characteristic of isolated iron ions in the glassy matrix. After annealing the glass, considerable changes arise in the spectra, as shown in figure 1. As T_a increases from 460 to 550 °C the $g_{ef} = 4.3$ line gradually decreases in intensity and finally disappears. Simultaneously, a narrow line emerges at $g_{ef} \approx 2.0$, superposed with a broader one. The narrow component predominates at lower anneal temperatures and, as T_a is further increased, it is progressively replaced by the broader one. Annealing above 550 °C results in a further transformation of the spectrum (not shown here). The narrow $g_{ef} \approx 2.0$ component disappears at $T_a = 670\,^{\circ}C$. Good reproducibility of spectra transformation as a function of the anneal temperature has been observed.

Numerical integration of the experimental (derivative-of-absorption) spectra yields the resonance absorption curves shown in figures 2 and 3. It is seen that at lower anneal temperatures the intensity of the $g_{ef} \approx 2.0$ signal gradually increases at the expense of the

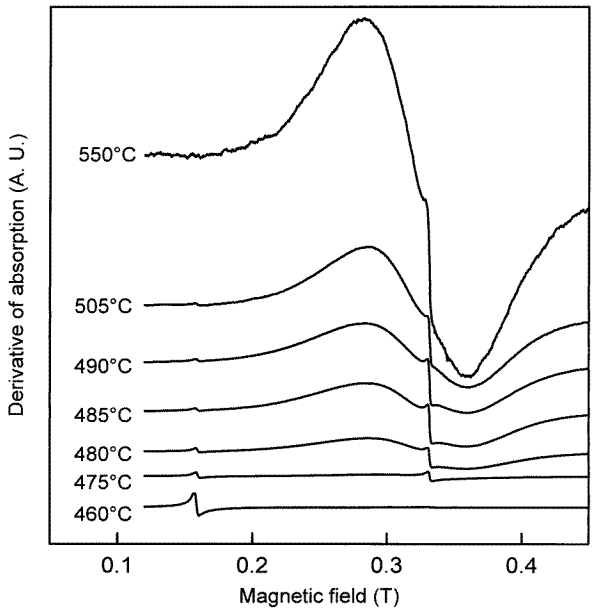

Figure 1. X-band room-temperature spectra recorded after repeated anneal steps for 0.5 h at temperatures T_a indicated on the curves.

$g_{ef} = 4.3$ resonance. At higher anneal temperatures the contribution of both the $g_{ef} = 4.3$ resonance and the narrow $g_{ef} \approx 2.0$ line becomes negligible in comparison with that of the broader $g_{ef} \approx 2.0$ signal which rapidly increases with T_a, see figure 3.

The total number of spins (in relative units) obtained by a second integration of the spectra is shown in figure 4. A continuous rapid growth of the detected number of spins takes place in the range of T_a of 475–550 °C. In this range, for a 10 °C increase in T_a the relative number of spins increases by ∼12%.

3. Computer simulations

3.1. Theoretical background

The characteristics of SPR of fine magnetic particles depend on the nature of the particles, on their geometry (shape and size) as well as on the applied magnetic field $\boldsymbol{B}_0$.

The experimental signal is proportional to the imaginary part of the first derivative of the dynamic susceptibility. On a microscopic level, this signal depends on the orientation of $\boldsymbol{B}_0$ with respect to the local magnetic axes. In a ferromagnetically ordered system all individual spins are coupled by an exchange interaction, which in bulk materials is described by the spontaneous magnetization $\boldsymbol{M}_s$.

We consider an assembly of fine single crystal ferromagnetic nanoparticles isolated in a diamagnetic matrix. Particles of relatively greater sizes may incorporate several magnetic domains; however, smaller particles are single domain [2]. In the latter case, the magnetization is related to the magnetic moment $\boldsymbol{m}$ of such a particle by

$$\boldsymbol{M}_s = \boldsymbol{m}/V \tag{1}$$

V being the particle volume. In a single-domain particle all individual spins are exposed

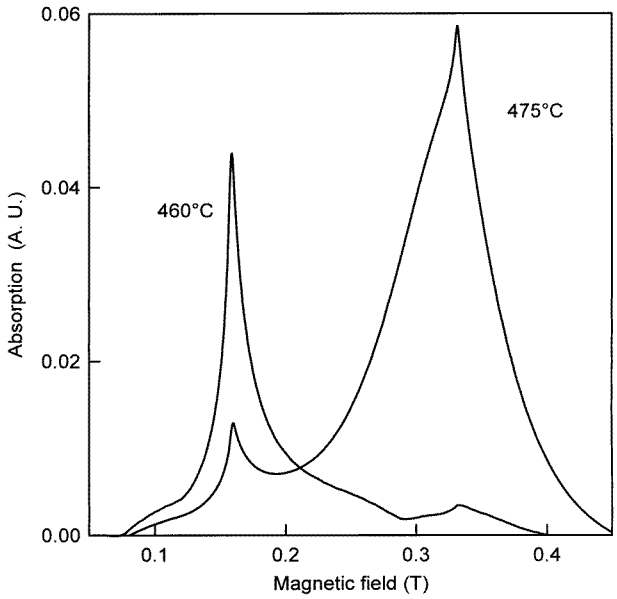

Figure 2. Absorption spectra at lower anneal temperatures (as indicated).

to the same conditions, so that such a particle will give rise to a SPR signal proportional to the number of spins inside the particle, that is, to its volume.

The equilibrium orientation of the $\boldsymbol{M}_s$ vector must minimize the free energy of the particle. This means that in thermodynamic equilibrium $\boldsymbol{M}_s$ is parallel to the effective magnetic field which includes, besides $\boldsymbol{B}_0$, a magnetocrystalline anisotropy field $\boldsymbol{B}_a$ and a demagnetizing field $\boldsymbol{B}_d$. In the absence of $\boldsymbol{B}_0$, in a spherical particle $\boldsymbol{M}_s$ is oriented along an easy axis of magnetization. On the other hand, in a strong external magnetic field case, typical of an electron magnetic resonance experiment, the Zeeman coupling between $\boldsymbol{M}_s$ and $\boldsymbol{B}_0$ dominates over all other interactions, so that in the first approximation, the orientation of $\boldsymbol{M}_s$ approaches that of $\boldsymbol{B}_0$ [8].

One assumes, in addition, that the particles are ellipsoids whose principal axes coincide with one of the local magnetic axes. In this approximation, the expression for the resonance magnetic field B_r becomes

$$B_r = B_0 + B_a + B_d \tag{2}$$

where B_a and B_d are projections of the respective vectors on the $\boldsymbol{B}_0$ direction defined by ϑ and φ, the polar and azimuthal angles. $\boldsymbol{B}_a$ is the magnetocrystalline anisotropy field expressed as

$$B_{a_{(C)}} = \frac{2K_{1(C)}}{M_s}[5(\sin^2\vartheta\cos^2\vartheta + \sin^4\vartheta\sin^2\varphi\cos^2\varphi) - 1] \tag{3}$$

for cubic symmetry crystals [8] and it can be easily shown that

$$B_{a_{(A)}} = \frac{K_{1(A)}}{M_s}(3\cos^2\vartheta - 1) \tag{4}$$

for axial symmetry crystals, where $K_{1(C)}$ and $K_{1(A)}$ are respectively the cubic and axial first-order anisotropy constants.

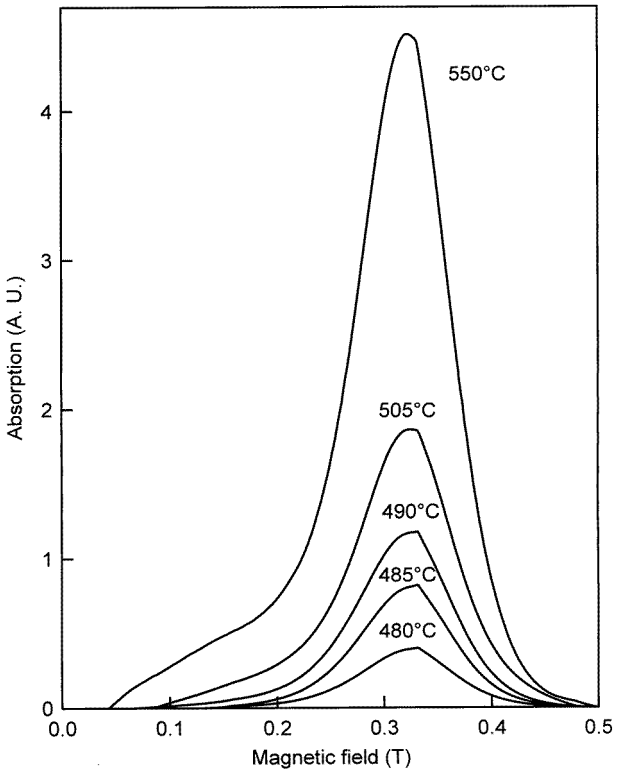

Figure 3. Absorption spectra at higher anneal temperatures (as indicated).

Assuming the particle shape as an ellipsoid of revolution, the demagnetizing field B_d in equation (2) becomes

$$B_d = \frac{\mu_0 M_s}{2}(N_\parallel - N_\perp)(3\cos^2\vartheta - 1) \tag{5}$$

where $N_\parallel$ and $N_\perp$ are demagnetization factors for the directions respectively parallel and perpendicular to the major axis of the ellipsoid.

The superparamagnetic behaviour is observed for fine particles with diameters less than $\sim$20 nm [2]. The magnetic moment of such a particle is subject to thermal fluctuations resulting in motional narrowing of the SPR spectra. The resonance magnetic field B_r, instead of equation (2), is now given by

$$B_r = B_0 + B_a^{sp} + B_d^{sp} \tag{6}$$

where B_a^{sp} is the superparamagnetic anisotropy field and B_d^{sp} is the superparamagnetic demagnetizing field. De Biasi and Devezas [9] have shown that B_a^{sp} can be expressed by means of the Langevin function $L(x) = \coth x - 1/x$, where $x = M_s B_r V/kT$, as follows:

$$B_{a(C)}^{sp} = B_{a(C)}\left[\frac{1}{L(x)} - \frac{10}{x} + \frac{35}{x^2 L(x)} - \frac{105}{x^3}\right] \tag{7}$$

or

$$B_{a(A)}^{sp} = B_{a(A)}\left[\frac{1}{L(x)} - \frac{3}{x}\right] \tag{8}$$

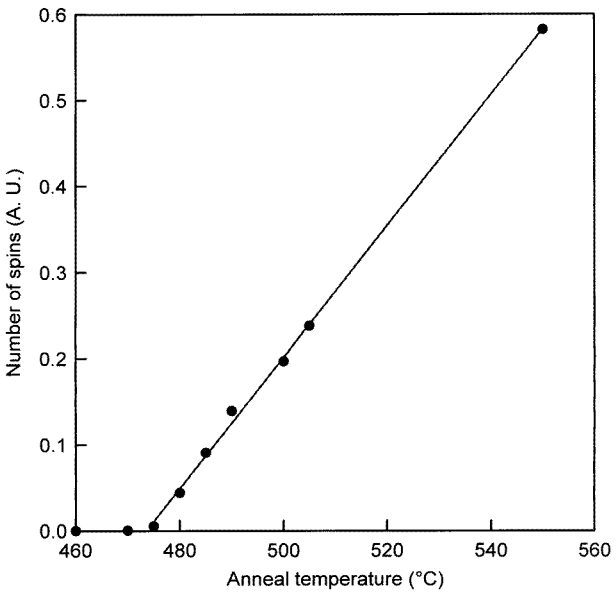

Figure 4. Number of spins (in relative units) in magnetic particles as a function of T_a. The straight line indicates a linear dependence in the range 475–550 °C.

respectively for crystallites with cubic or axial symmetry. The B_d^{sp} field can be written as

$$B_d^{sp} = B_d L(x). \tag{9}$$

Next one must take into account that for a disordered assembly of magnetic particles, for example for particles formed by crystallization and clustering of iron oxide-based structural units in a glass matrix, distributions of sizes and shapes may arise. Several authors have shown that if the particle shape is close to a sphere, the log–normal diameter distribution is the most appropriate one, for example in the case of demixing processes of glasses during heat treatment [10, 11] or for fine magnetic particles dispersed in a fluid (ferrofluids) [12–14]. A number of interrelated expressions of the probability density $P(D)$ of finding a particle with a diameter D can be used [13]. The most current one is

$$P(D) = \frac{1}{\sqrt{2\pi}\sigma D} \exp\left[-\frac{1}{2\sigma^2} \ln^2 \frac{D}{D_0}\right] \tag{10}$$

with σ the standard deviation of $\ln D$ and D_0 defined by $\ln D_0 = \langle \ln D \rangle$. D_0 is related to the most probable particle diameter D_m, corresponding to the maximum of $P(D)$, by

$$D_m = D_0 \exp(-\sigma^2). \tag{11}$$

Then (10) can also be written as

$$P(D) = \frac{\exp(-\sigma^2/2)}{\sqrt{2\pi}\sigma D_m} \exp\left[-\frac{1}{2\sigma^2} \ln^2 \frac{D}{D_m}\right]. \tag{12}$$

The mean particle diameter is calculated as

$$\langle D \rangle = D_m \exp(\tfrac{3}{2}\sigma^2) = D_0 \exp(\tfrac{1}{2}\sigma^2). \tag{13}$$

It can easily be shown [14] that in this case the probability density of the volume fraction of particles with a diameter D is also a log–normal one, with the same σ,

$$f_V(D) = \frac{\exp(-\sigma^2/2)}{\sqrt{2\pi}\,\sigma\, D_{Vm}} \exp\left[-\frac{1}{2\sigma^2}\ln^2\frac{D}{D_{Vm}}\right] \tag{14}$$

where D_{Vm} corresponds to the maximum of $f_V(D)$. D_{Vm} is related to D_m by

$$D_{Vm} = D_m \exp(3\sigma^2). \tag{15}$$

The SPR spectrum of an assembly of particles described by the distribution equation (14) can be calculated as

$$I(B) = \int_\varphi \int_\vartheta \int_D F[B - B_r(D, \vartheta, \varphi), \Delta B] f_V(D) \sin\vartheta \,\mathrm{d}D \,\mathrm{d}\vartheta \,\mathrm{d}\varphi \tag{16}$$

with the lineshape function $F[B - B_r(D, \vartheta, \varphi), \Delta B]$ which can be taken as Lorentzian or Gaussian (the latter provides a better fit in the present case), ΔB being the individual linewidth for a particle of a given size.

With increasing particle volume, the SPR linewidth has been found to increase for the finest particles and decrease above a certain size [4]. Other workers, for example see [15], have put forward a linewidth dependence which can approximately be written as

$$\Delta B = \Delta B_T \tanh(x) \tag{17}$$

where ΔB_T is the saturation linewidth at a given temperature (presumably due to magnetic interactions between the particles). The $\tanh(x)$ factor in equation (17) is related to thermally-induced jumps between two available states corresponding to two distinct orientations with respect to the easy axis of magnetization. Note that a dependence analogous to equation (17) has been found for the interaction field in a system of weakly interacting magnetic particles [16]. However, in a more refined model, for a disordered assembly of particles with distributed volumes [17], the Langevin function $L(x)$ arises instead of the $\tanh(x)$. It seems that in the linewidth expression the use of $L(x)$ would also be a better choice. Indeed, $\tanh(x)$ is the Brillouin function corresponding to the spin $S = 1/2$, whereas the superparamagnetic particles can be considered as systems with $S \gg 1$, so that in the strong external magnetic field case a quasi-infinite number of orientations of $\boldsymbol{M}_s$ are possible with respect to any given axis. So, we have chosen for computer simulations the following linewidth expression:

$$\Delta B = \Delta B_T L(x). \tag{18}$$

Note that equation (18) has a similar form to the superparamagnetic demagnetizing field, equation (9).

3.2. Results

The exact chemical composition of the magnetic particles formed by heat treatment cannot be determined by direct structural studies. In low-level iron-doped borate glass these particles must certainly be related to some iron oxide or oxygen-containing salt, as this is the case for crystallites in borate glasses with high iron contents [18]. Moreover, data on magnetic constants of some oxygen-containing magnetic iron compounds possibly formed in crystallized borate do not seem to be available. In order to gain some insight into the possible nature of the magnetic particles, we have carried out a series of computer simulations of a representative room-temperature compound SPR signal recorded at room temperature after an anneal at $T_a = 480\,^\circ$C. The magnetic constants of three different compounds, magnetite

Fe_3O_4, maghemite γFe_2O_3 and lithium ferrite $LiFe_5O_8$ as given in table 1, have been used in the simulations. In each case the fitting has been attempted for both cubic and axial symmetries; the most satisfactory results are shown in figure 5.

Table 1. Magnetic constants of iron-containing compounds used in the simulations and the best-fit parameters obtained for the room-temperature SPR spectrum of glass annealed at $T_a = 480\,^{\circ}$C.

Compound	M_s (kA m^{-1})	K_1 (kJ m^{-3}) (C: cubic, A: axial)	Ref.	D_m (nm)	D_{Vm} (nm)	σ	ΔB_T (mT)
Fe_3O_4	478	−11 (C)	[20–22]	3.4	11.5	0.64	77
γFe_2O_3	370	−4.64 (C)	[21, 22]	3.7	12.5	0.64	79
γFe_2O_3	370	−4.64 (A)	[21, 22]	3.6	12.2	0.64	79
$LiFe_5O_8$	310	−8 (C)	[19]	4.0	13.3	0.63	78

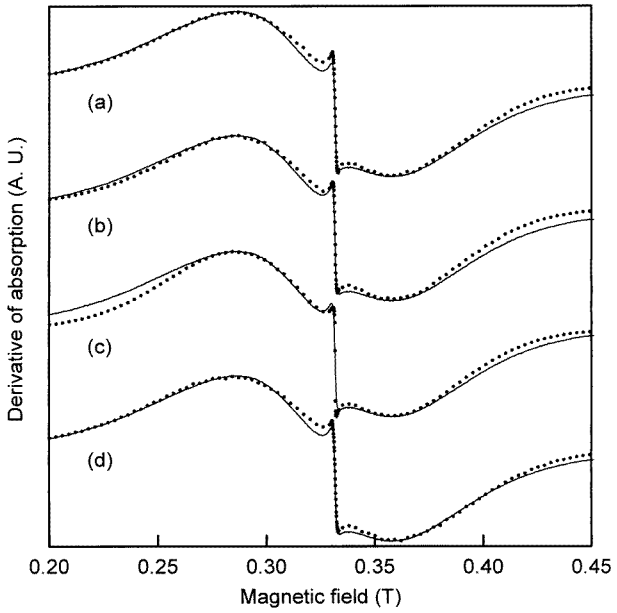

Figure 5. Computer simulations of the room-temperature spectrum for $T_a = 480\,^{\circ}$C with the data of table 1 (——, experiment; . . ., simulation): (a) Fe_3O_4 (cubic symmetry); (b) γFe_2O_3 (cubic symmetry); (c) γFe_2O_3 (axial symmetry); (d) $LiFe_5O_8$ (cubic symmetry).

In order to improve computer fitting, in particular in the low-field wings of the experimental spectra, linear relations between the demagnetization factors and the particle volume have been assumed.

In a rather surprising way, for cubic symmetry a good agreement between experimental and simulated SPR spectra has been obtained for all three cases. Assuming axial symmetry, convincing fits could be obtained only with the magnetic constants of maghemite. Table 1 shows the best-fit parameters obtained: the most probable diameter D_m, the diameter D_{Vm}, the standard deviation σ and the saturation linewidth ΔB_T.

From inspection of figure 5 and the values listed in table 1 it is seen that the computed spectra do *not* depend to a great extent on the nature of the magnetic particles. Indeed, in

the four cases summarized in table 1, in spite of quite different magnetic constants, very similar characteristic diameters and almost identical standard deviations are obtained, for close SPR linewidth values. It should be noted, however, that fitting to the experimental spectra implies a negative sign of the K_1 constant.

Finally, as it seems reasonable to assume that the crystallized fine particles are of the same nature in both low-iron-oxide- and high-iron-oxide-containing borate glasses, we have adopted for further computer simulations the magnetic parameters of lithium ferrite, the fine particles of which have recently been detected in annealed borate glasses with high iron content [19].

Figure 6 shows some of the experimental room-temperature SPR spectra recorded after repeated annealing steps at different T_a together with computer fits. Table 2 reports the values of the most probable particle diameter D_m and of the diameter D_{Vm} defined in equation (15).

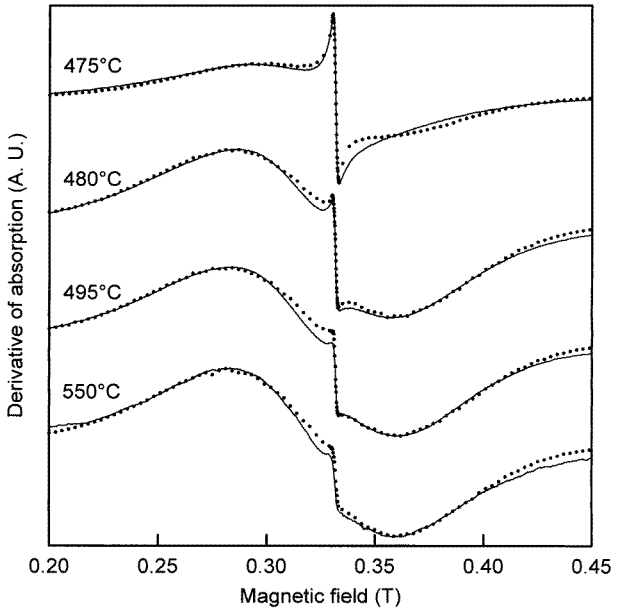

Figure 6. Computer simulations of the room-temperature spectra of borate glass annealed at different T_a obtained with magnetic constants of $LiFe_5O_8$, see table 1 (——, experiment; . . ., simulation).

4. Discussion

As shown earlier [3] for EPR spectra of low-concentration iron-oxide-doped borate glass, the $g_{ef} = 4.3$ arises from Fe^{3+} ions isolated in the vitreous network whereas the $g_{ef} \approx 2.0$ compound resonance is the signature of superparamagnetic particles imbedded in a more or less crystallized matrix, a vitreous phase persisting as long as the $g_{ef} = 4.3$ line is present.

At lower anneal temperatures when the magnetic particles begin to form, the intensity of the $g_{ef} = 4.3$ line decreases rapidly, see figure 2. This means that the number of Fe^{3+} ions in isolated heavily distorted low-symmetry sites is reduced. Any appreciable migration of Fe^{3+} ions can certainly be ruled out in this anneal temperature range. On the other

Table 2. Best-fit parameters obtained for room-temperature SPR spectra of glass annealed at different T_a (figure 6) using the magnetic constants of $LiFe_5O_8$ (see table 1).

T_a (°C)	D_m (nm)	D_{Vm} (nm)	σ	ΔB_T (mT)
475	2.9	9.7	0.63	78
480	4.0	13.3	0.63	78
485	4.2	13.7	0.63	78
490	4.3	14.0	0.63	78
495	4.3	14.2	0.63	78
505	4.5	14.7	0.63	74
550	4.7	15.5	0.63	74

hand, previous data on the EPR of Fe^{3+} ions in non-annealed borate glasses indicate a very inhomogeneous distribution of iron in the glass matrix [7]. Therefore, the modifications in the spectra observed at these stages are indicative of local structural transformations (ordering and reducing low-symmetry distortions) in the immediate surroundings of the iron sites which create precursors of crystallization.

The behaviour of the SPR absorption spectra at higher anneal temperatures is quite different, see figure 3. As the anneal temperature is increased, the SPR absorption intensity in the neighbourhood of $g_{ef} \approx 2$ grows very rapidly. Note that at these anneal stages the absorption at $g_{ef} = 4.3$ becomes negligible. One can conclude that the number of spins responsible for the $g_{ef} \approx 2$ absorption is rapidly increased with the anneal temperature (figure 4). In these circumstances, one might wonder if in the course of anneal the total number of spins in the sample remains constant. Fe^{2+} ions in borate glasses are present only in a small amount (typically 5% of the total number of iron ions [23]), so that their possible transformation into Fe^{3+} could not account for the apparent increase in the number of spins in the course of anneal.

The most likely explanation of this 'paradox' is related to the complex nature of the $g_{ef} = 4.3$ resonance in glass. This line originates from the middle Kramers doublet of magnetically isolated Fe^{3+} ions described by the spin Hamiltonian

$$\mathcal{H} = g\beta \boldsymbol{B} \cdot \boldsymbol{S} + D[S_z^2 + \tfrac{1}{3}S(S+1)] + E(S_x^2 - S_y^2) \tag{19}$$

in a strong orthorhombic symmetry crystal field, $|D| > g\beta B$, $\lambda = E/D \approx 1/3$ [24] and the effective g-values of the three Kramers doublets as function of D and λ may vary between 0 and 10 so that the paramagnetic absorption is spread over a very broad magnetic field range. By computer simulating this resonance in borate glass [6], we have shown previously that the D and λ parameters are largely distributed. It follows that the features observed in the experimental EPR spectrum and well reproduced by simulation (the $g_{ef} = 4.3$ sharp line and the much weaker shoulder at $g_{ef} = 9.7$) arise only from the small part of the total number of Fe^{3+} ions whose magnetic parameters satisfy the above-mentioned conditions on D and λ. The majority of isolated Fe^{3+} ions in this instance give rise to a featureless background absorption spreading well beyond the scan range of the spectrometer. Appropriate computer simulations show that this absorption is completely lost in the noise. As meaningful integration of experimental derivative-of-absorption spectra can be performed only over the magnetic field range where distinct features are observed, the latter absorption cannot be detected in this way. So, the apparent total absorption intensity is not conserved in the course of spectra transformations.

On the other hand, as far as the integrated absorption of only the $g_{ef} \approx 2.0$ resonance is concerned, there is no doubt that its intensity is directly proportional to the total number of

spins inside the magnetic particles, that is, to the total volume thereof (figure 4). The evolution with the anneal temperature of the most probable diameter D_m is shown in figure 7(a) and that of the corresponding volume $V_m = \frac{1}{6}\pi D_m^3$ in figure 7(b). From a comparison of the figures 4 and 7(b), one can see that the total volume of the magnetic particles is not proportional to the volume corresponding to the most probable diameter, so that the number of particles certainly does not remain constant in the course of the anneal.

At lower anneal temperatures, ∼460–480 °C, the most probable diameter of the magnetic particle increases rapidly, while at higher ones, ∼480–550 °C, this increase is slowed down,

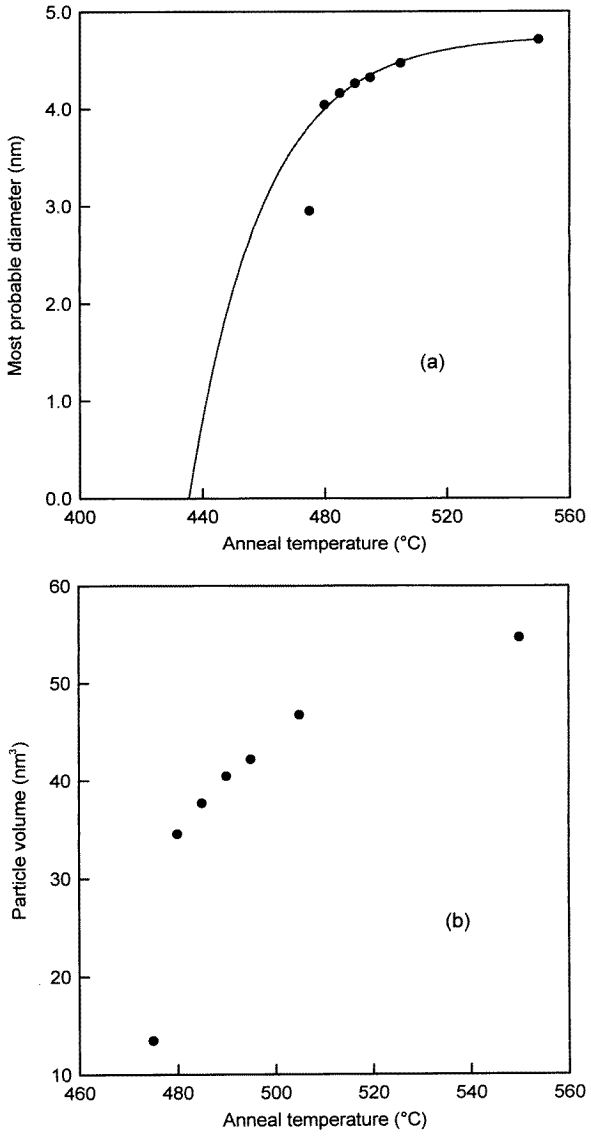

Figure 7. The most probable diameter D_m (a) and the corresponding particle volume (b) for different T_a. The full curve in (a) corresponds to equation (20).

see figure 7. On the other hand, the total volume of the particles continues to grow, see figure 4, so that the number of the larger particles rapidly increases.

Note that convincing computer fits have been obtained with only a small number of adjustable parameters. One can see from table 2 that with the increase of the anneal temperature the most probable diameter grows while the standard deviation (the distribution width) and the saturation linewidth remain nearly constant. The values of D_{Vm} determined by SPR are in good agreement with particle sizes obtained by other methods in annealed glasses [19, 25, 26] and in other materials, such as ferrofluids [14, 22, 27, 28]. The σ values obtained in this study for the magnetic particles in borate glass are larger than those generally found for ferrofluids (0.2–0.5) [12, 22], but smaller than that reported for a sodium silicate glass ($\approx$1.4) [25].

To summarize, we show in figure 8 the dependence of the relative number of particles on their diameter for different anneal temperatures. One can conclude that the most significant characteristic feature of the transformations arising in the course of the repeated annealing stages of the glass is a very rapid increase in the particle number and a much slower increase in the most probable diameter, the overwhelming majority of particles having a diameter between about 2 and 12 nm.

Figure 8 provides some evidence on the mechanism of formation of the magnetic particles. It is seen, figure 13 of [10], that in the present case the larger particles do not grow at the expense of the smaller ones, so that the Ostwald ripening mechanism can be ruled out. The quasi-linear increase in the total number of spins with anneal temperature up to 550 °C, see figure 4, suggests that the Fe^{3+} ions are continuously incorporated into magnetic particles (continuous crystallization).

Figure 7 gives other evidence on the mechanism of particle growth. One can see that at higher anneal temperatures, ~480–550 °C, the dependence on T_a of the most probable

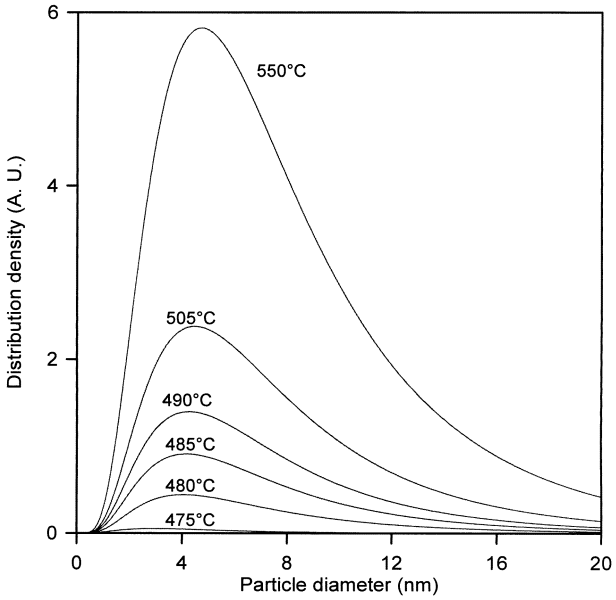

Figure 8. The distribution density of the number of particles as a function of their diameters for different T_a.

particle diameter can be well approximated by the following empirical formula,

$$D_m = D_{mM}\left(1 - \exp\frac{T_{a0} - T_a}{\Theta}\right) \tag{20}$$

where $D_{mM} = 4.75$ nm is the limiting value of the most probable diameter reached by anneal, with $T_{a0} = 435.5\,^{\circ}\mathrm{C} \approx T_g$, T_g being the glass transition temperature and Θ some characteristic temperature. This relation infers the existence, in the conditions of anneal used, of a limiting size of superparamagnetic single-domain particles. A further growth of the particles would certainly result in a multi-domain structure minimizing the magnetostatic energy. On the other hand, equation (20) implies that the formation of crystallized particles begins at the glass transition temperature. Note, however, that the experimental points in figure 7 follow equation (20) only for anneal temperatures considerably higher than the exact T_g value.

A relation between the demagnetization factors and the particle volume used in order to improve the fits, *vide ultra*, suggests a more pronounced ellipticity for particles of a greater volume. It may, however, be rather an artefact related, for example, to the volume dependence of the superparamagnetic demagnetizing field, which may be different from that of equation (9), or to the particle surface characteristics (which are not taken into account in the present model).

5. Conclusion

Successful computer simulations of electron magnetic resonance spectra of superparamagnetic nanoparticles in annealed borate glass have been carried out. The simulated spectra are much more sensitive to the size distribution of the particles than to the choice of magnetic constants of the compound constituting them. The characteristic diameter values determined assuming a log–normal distribution of the particle diameters are in good agreement with the results obtained by other methods for some similar systems.

As the anneal temperature increases, in the actual anneal conditions the total volume of the magnetic nanoparticles grows linearly. On the other hand, the most probable particle diameter increases very rapidly at lower anneal temperatures, and shows a tendency towards saturation at higher anneal temperatures so that the number of larger particles is increased at this stage.

Some important features of nanoparticles have been neglected in the present study, such as their surface characteristics or relaxation times associated with the thermal fluctuations of the magnetic domains. Nevertheless, quite consistent results have been obtained, concerning the geometrical characteristics of the magnetic nanoparticles at different anneal temperatures of the glass.

In conclusion, the present study shows that the electron magnetic resonance in association with computer simulations yields an effective tool for exploring the morphology of magnetic nanoparticles in superparamagnetic systems.

References

[1] Doremus R H 1973 *Glass Science* (New York: Wiley) p 74
[2] Dormann J L, Fiorani D and Tronc E 1997 Magnetic relaxation in fine-particles systems *Advances in Chemical Physics* vol 98, ed I Prigogine and S A Rice (New York: Wiley)
[3] Berger R, Bissey J-C, Kliava J and Soulard B 1997 *J. Magn. Magn. Mater.* **167** 129
[4] Dubowik J and Baszynski J 1986 *J. Magn. Magn. Mater.* **59** 161
[5] Raikher Yu L and Stepanov V I 1995 *J. Magn. Magn. Mater.* **149** 34

[6] Yahiaoui E M, Berger R, Servant Y, Kliava J, Cugunov L and Mednis A 1994 *J. Phys.: Condens. Matter* **6** 9415
[7] Berger R, Kliava J, Yahiaou E-M, Bissey J-C, Zinsou P-K and Béziade P 1995 *J. Non-Cryst. Solids* **180** 151
[8] Schlömann E J 1958 *Phys. Chem. Solids* **6** 257
[9] de Biasi S and Devezas T C 1978 *J. Appl. Phys.* **49** 2466
[10] Zarzycki J and Naudin F 1967 *Phys. Chem. Glasses* **8** 11
[11] Zarzycki J 1974 *J. Appl. Crystallogr.* **7** 200
[12] Bacri J-C, Boué F, Cabuil V and Perzynski R 1993 *Colloids Surfaces* A **80** 11
[13] Upadhyay R V, Sutariya G M and Mehta R V 1993 *J. Magn. Magn. Mater.* **123** 262
[14] Popplewell J and Sakhnini L 1995 *J. Magn. Magn. Mater.* **149** 72
[15] Morais P C, Lara M C L and Skeff Neto K 1987 *Phil. Mag. Lett.* **55** 181
[16] Shtrikman S and Wohlfarth E P 1981 *Phys. Lett.* **85A** 467
[17] Dormann J L, Bessais L and Fiorani D 1988 *J. Phys. C: Solid State Phys.* **21** 2015
[18] Laville H and Bernier J C 1980 *J. Magn. Magn. Mater.* **15–18** 193
[19] Rezlescu E, Rezlescu N and Craus M L 1997 *J. Physique* IV **7** C1 553
[20] Margulies D T, Parker F T and Berkowitz A E 1994 *J. Appl. Phys.* **75** 6097
[21] Schmidbauer E and Keller R 1996 *J. Magn. Magn. Mater.* **152** 99
[22] Gazeau F 1997 *Thesis* Université Paris 7
[23] Zhang Z 1993 *Phys. Chem. Glasses* **34** 77
[24] Wickman H H, Klein M P and Shirley D A 1965 *J. Chem. Phys.* **42** 2113
[25] Roy S, Roy B and Chakravorty D 1996 *J. Appl. Phys.* **79** 1642
[26] Estournès C, Lutz T, Happich J, Quaranta P, Wissler P and Guille J L 1997 *J. Magn. Magn. Mater.* **173** 83
[27] Dormann J L, d'Orazio F, Lucari F, Tronc E, Prené P, Jolivet J P, Fiorani D, Cherkaoui R and Noguès M 1996 *Phys. Rev.* B **53** 14 291
[28] Feltin N and Pileni M P 1997 *J. Physique* IV **7** C1 609